Enhanced light extraction from circular Bragg grating coupled microcavities

Mark Y. Su[a] and Richard P. Mirin
National Institute of Standards and Technology, 325 Broadway, Boulder, Colorado 80305

(Received 21 December 2005; accepted 13 June 2006; published online 18 July 2006)

A sevenfold enhancement of light extraction over a 130 nm bandwidth from a semiconductor at room temperature was achieved using circular Bragg gratings (CBGs) etched around the periphery of a vertical-cavity light-emitting structure. The CBG defined an in-plane circular cavity for light trapped in guided modes. Maximum enhancement was observed with CBGs that efficiently coupled circular cavity modes into resonant extracted modes of the vertical cavity. The enhancement factor corresponded to a 41% external efficiency. [DOI: 10.1063/1.2222345]

Semiconductor light-emitting diodes (LEDs) can efficiently generate light throughout the ultraviolet, visible, and near-infrared spectra. Unfortunately, because of the high index mismatch at the semiconductor-air interface, only ~2% of the light in a conventional LED is extracted within a narrow ~18° cone normal to the surface. The remaining light is emitted into the substrate, or trapped and reabsorbed in the active layer. The development of nanophotonic structures such as photonic crystals to enhance light extraction[1–4] could offer superior efficiency, integration, and cost over present efforts in LED chip shaping and packaging.

The integration of a distributed Bragg reflector (DBR) behind the active region can enhance light extraction for resonant modes of the vertical cavity between the air interface and the DBR.[5] Forming the DBR using materials with high index contrast, such as GaAs and AlO_x, creates broadband reflectivity over the entire range of angles comprising the light extraction cone.[6] Light emitted outside the extraction cone is trapped in guided modes that never exit the surface.

To extract guided modes, we incorporated circular Bragg gratings (CBGs) etched to form the perimeter of 20 μm circular cavities (Fig. 1). Diffraction from the gratings provided the momentum transfer necessary to couple the in-plane circular cavity modes to extracted modes of the vertical cavity. The etched grating on the periphery of the light-emitting mesa did not spoil the internal quantum efficiency through surface recombination, as has been the case with photonic crystals etched into the same region where radiative recombination occurs.[4]

The sample, grown by molecular beam epitaxy, consisted of three layers of InGaAs self-assembled quantum dots in the center of a 300 nm thick GaAs spacer layer. The quantum dot layers were spaced by 12 nm. Below the spacer layer was a four period $GaAs/AlO_x$ DBR with high reflectance centered at 1110 nm. The oxide layers were formed from the native oxide of epitaxial $Al_{0.9}Ga_{0.1}As$ during processing.

The CBGs were written into 250 nm thick polymethyl methacrylate (PMMA) with electron beam lithography. The developed PMMA was used as a mask for subsequent chlorine-assisted ion-beam etching resulting in smooth, vertical sidewalls 150 nm deep through the active layer. A trench around the CBG was then wet etched through the DBR with a phosphoric acid mixture. The DBR was then laterally wet oxidized in a steam furnace.

The devices were optically pumped with an 810 nm laser diode focused with a 0.55 numerical aperture (NA) 20× objective. The 5 μm diameter pump spot was focused on the center of the devices at a maximum excitation power of 1 mW. The collected photoluminescence (PL) was dispersed with a 0.3 m spectrometer with a 300 groove/mm grating and detected with an InGaAs photodiode array.

We collected 17 nW of PL from the unpatterned, unoxidized sample at 1 mW incident pump power. The wavelength-integrated PL from an oxidized device with no CBG had a 2.7× enhancement over the PL from an unoxidized sample, demonstrating the role of the vertical cavity in enhancing light extraction. Devices with 525 nm (Fig. 2, red) and 360 nm (Fig. 2, green) pitch CBGs showed large PL enhancements over a device with no CBG. Resonant enhancement was as high as 11.9× at 1137 nm. The sharp peaks in the PL spectra corresponded to the guided modes that satisfied the in-plane resonances of the 20 μm diameter circular cavity (CC), with an 8.5 nm average free spectral range. As the PL intensity was linear with pump power at all wavelengths, we observed no amplified spontaneous emission.

The far-field radiation pattern was characterized[7] with a variable aperture after the collection objective and a scanning spatial filter before the spectrometer input. The radiation pattern of the 1148 nm peak from the 525 nm pitch CBG was

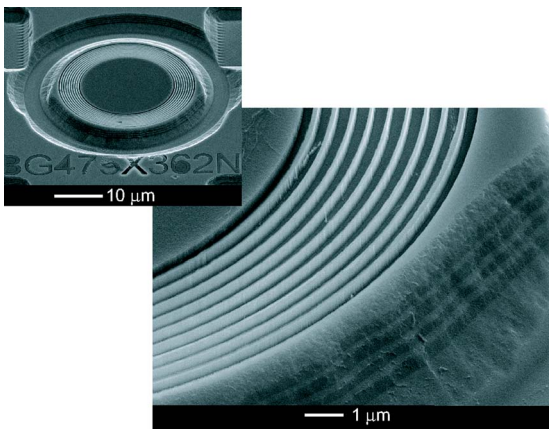

FIG. 1. Scanning electron micrograph of circular Bragg grating device. The outer trench was for lateral oxidation of the DBR mirror layers, visible in the lower right corner of the zoom.

[a]Electronic mail: marksu@boulder.nist.gov

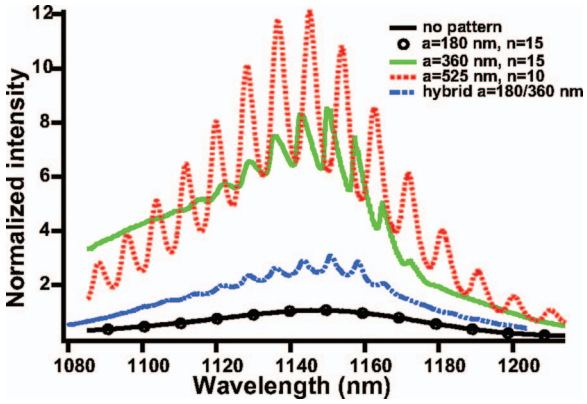

FIG. 2. (Color) In order of increasing intensity: PL spectra for devices with no grating, a 180 nm CBG, a hybrid 180 nm/360 nm CBG, a 360 nm CBG, and a 525 nm CBG. The PL of the 180 nm CBG was indistinguishable from the PL of a device with no grating. n is the number of periods.

single lobed with a divergence angle of 18° and a waist diameter of 40 μm.

The dispersion (Fig. 3) of the planar waveguide modes was calculated using a transfer matrix formalism.[8] There is a guided mode (GM) in the GaAs spacer layer (Fig. 3, blue), a guided mode for each GaAs layer in the DBR (Fig. 3, green), and a resonant extracted mode (REM) of the vertical cavity (VC) (Fig. 3, red). Nonresonant radiation modes (NRRMs) form a continuum above the light line. The REM lies above the light line but is mostly confined to the spacer layer.[5] Figures 3(b) and 3(c) show the guided mode and resonant extracted modes as bands folded into the first Brillouin zone for various pitch gratings. Overlapping bands match momenta and will have nonzero coupling. Guided modes folded above the light line overlap with nonresonant radiation modes. The intersection of positively and negatively sloped bands corresponds to the standing waves of the CC.

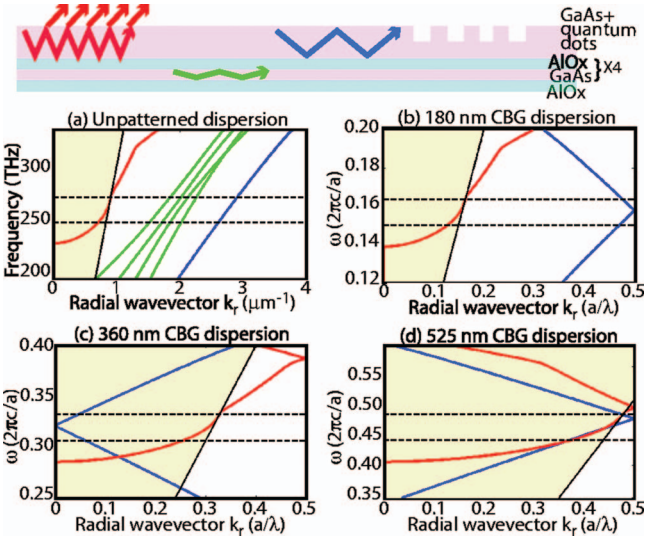

FIG. 3. (Color) Top: diagram of resonant extracted mode (REM) confined to spacer layer (red), guided modes in the DBR GaAs layers (green), and guided mode in the spacer layer (blue). Mode color scheme is the same for dispersion diagrams (a)–(d), with DBR guided modes omitted for clarity. (a) Dispersion diagram of unpatterned device showing nonresonant radiation mode (NRRM) continuum above light line shaded in yellow. [(b)–(d)] First Brillouin zones for CBG periodicities of 180, 360, and 525 nm. Horizontal dotted lines bound the experimental frequency range. Light emitted in shaded region between horizontal dotted lines is extracted and collected.

A 180 nm pitch grating [Fig. 3(b)] folds no additional modes above the light line. Therefore, we would expect that the first-order CBG would display no enhancement of PL extraction. As expected, the first-order CBG PL was indistinguishable from the PL with no grating (Fig. 2, black).

For the 360 nm pitch grating [Fig. 3(c)] the CC standing wave is formed at the zone center and thus coupled to nonresonant radiation modes with nearly no in-plane momentum (near-normal propagation). Thus, we observe the large enhancement of PL intensity and the appearance of CC modes in the spectrum. Interestingly, when a 360 nm grating was added to the outside of the 180 nm grating, the CC modes defined by the 180 nm grating were recovered (Fig. 2, blue). Such a hybrid grating configuration could be useful in fabricating high-Q surface-emitting microcavities.

The 525 nm pitch grating neatly folds the guided mode on top of the resonant extracted mode in the frequency range of interest [Fig. 3(d)]. GM-NRRM coupling and GM-REM coupling require not only matched momenta but also nonzero overlap between the mode envelopes. In the GM-REM case both modes are confined to the vertical cavity. Therefore the GM-REM overlap integral can be much greater than the GM-NRRM overlap integral. The enhancement of the GM-REM overlap relative to the GM-NRRM overlap is approximately equal to the enhancement of the REM electric field within the vertical cavity:[9]

$$\frac{\left|\int_{-d}^{+\infty}\Phi_{\mathrm{GM}}(z)\Phi_{\mathrm{REM}}(z)dz\right|}{\left|\int_{-d}^{+\infty}\Phi_{\mathrm{GM}}(z)e^{-ik_z z}dz\right|}\approx\frac{|E_{\mathrm{REM}}|}{|E_{\mathrm{NRRM}}|}=\frac{1}{1-|r(k_r)|},\quad(1)$$

where d is the etch depth with $z=0$ at the sample surface, $\Phi_{\mathrm{GM}}(z)$ and $\Phi_{\mathrm{REM}}(z)$ are, respectively, the guided and resonant extracted mode envelopes, $e^{-ik_z z}$ is the z dependence of the nonresonant radiation mode, $|E_{REM}|/|E_{NRRM}|$ is the ratio of electric field strengths of the resonant extracted and nonresonant radiation modes within the active layer, and $r(k_r)$ is the Fresnel reflection coefficient at the GaAs-air interface for a resonant extracted wave with in-plane radial wave vector k_r. The calculated coupling-coefficient enhancement of the REM over a NRRM can be large: at 1145 nm it is a factor of 8.

The inset in Fig. 4 shows the PL spectra for 360 nm pitch CBGs with a varying number of periods. As periods were added, overall light extraction was enhanced and CC modes became more distinct. The integrated light extraction from the 360 nm CBGs and 525 nm CBGs is compared in Fig. 4. We measured an extraction enhancement up to 7.5× integrated over the 130 nm bandwidth. We estimated the extraction efficiency[5] of a device with no CBG as $\sim 2.7/4n^2 = 0.055$, where $n=3.5$ is the GaAs refractive index and the factor of 2.7 is the measured enhancement from the oxidized DBR. Therefore an enhancement of 7.5× corresponded to an absolute external efficiency of the CBG device of ~41%.

Clearly the 525 nm CBGs were strongly coupled, while the 360 nm CBGs were weakly coupled. The difference in coupling can be attributed to the enhanced overlap described by Ref. 1. The relative additional light extractions for two CBGs with n periods were calculated by

$$I_{525}(n)=A\int d\lambda N(\lambda)[1-e^{-(5.25\times10^{-5}\ \mathrm{cm})\alpha n/1-r_l(\lambda)}],\quad(2)$$

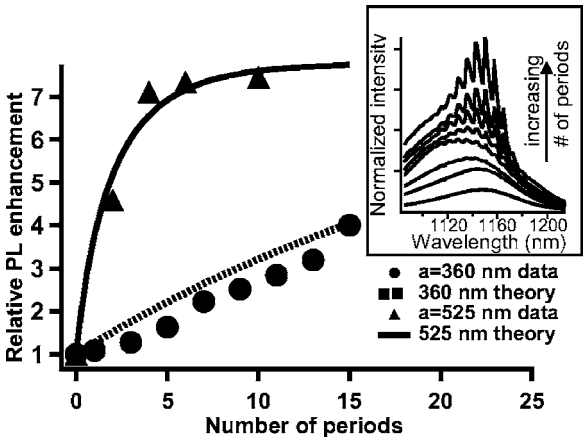

FIG. 4. Integrated PL intensity vs number of grating periods for 525 nm pitch and 360 nm pitch CBGs. Solid line is theoretical fit to 525 nm data using Eq. (2). Dotted line is Eq. (3) using parameters based on the fit to Eq. (2). Inset: PL spectra for 360 nm pitch CBG with varying number of periods.

$$I_{360}(n) = A \int d\lambda N(\lambda)[1 - e^{-(3.60\times10^{-5}\ \mathrm{cm})\alpha n}], \qquad (3)$$

where $r_l(\lambda)$ is the calculated Fresnel reflection coefficient for the resonant extracted mode and $N(\lambda)$ is the population of quantum dots emitting at λ, given by a Gaussian fit to the unpatterned PL intensity. The free scaling parameters α and A were obtained by fitting (2) to the 525 nm CBG data in Fig. 4. Physically, A (in milliwatts) scales with the total power available in the guided mode, while α (cm^{-1}) scales with the absolute value of the coupling coefficient and is a complicated function of the high index contrast grating profile.[10] Plugging A and α into (3) resulted in close agreement with the 360 nm CBG data.

In conclusion, a sevenfold enhancement of light extraction over a 130 nm bandwidth from a semiconductor at room temperature was achieved using CBGs etched around the periphery of a VC. A CBG defined an in-plane CC for light trapped in guided modes. Large light extraction enhancement was observed with CBGs that coupled guided CC modes to nonresonant radiation modes. Mode extraction was maximized by near-perfect momentum matching of the guided CC modes with REMs of the VC, as modal overlap was enhanced by the relative confinement of the REM. The calculated absolute external efficiency of the CBG device was ~41%.

[1] A. A. Erchak, D. J. Ripin, S. Fan, P. Rakich, J. D. Joannopoulos, E. P. Ippen, G. S. Petrich, and L. A. Kolodziejski, Appl. Phys. Lett. **78**, 563 (2001).
[2] M. Rattier, H. Benisty, R. P. Stanley, J.-F. Carlin, R. Houdre, U. Oesterle, C. J. M. Smith, C. Weisbuch, and T. F. Krauss, IEEE J. Quantum Electron. **8**, 238 (2002).
[3] H. Ichikawa and T. Baba, Appl. Phys. Lett. **84**, 457 (2004).
[4] H. Y. Ryu, Y. H. Lee, R. L. Sellin, and D. Bimberg, Appl. Phys. Lett. **79**, 3573 (2001).
[5] H. Benisty, H. De Neve, and C. Weisbuch, IEEE J. Quantum Electron. **34**, 1612 (1998).
[6] D. L. Huffaker, C. C. Lin, J. Shin, and D. G. Deppe, Appl. Phys. Lett. **66**, 3096 (1998).
[7] Following International Standard ISO 11146–1:2005.
[8] J. Chilwell and I. Hodgkinson, J. Opt. Soc. Am. A **1**, 742 (1984).
[9] R. F. Kazarinov and C. H. Henry, IEEE J. Quantum Electron. **QE-21**, 144 (1985). Using step-function coupling constant $\alpha(z)$ for square grating.
[10] J. Scheuer and A. Yariv, J. Opt. Soc. Am. B **20**, 2285 (2003).